Direct Estimation of the Electron Diffusion Length in Dye-Sensitized Solar Cells

ARTICLE *in* JOURNAL OF PHYSICAL CHEMISTRY LETTERS · APRIL 2011

Impact Factor: 7.46 · DOI: 10.1021/jz200340h

9 AUTHORS, INCLUDING:

Rodrigo Alcántara
Universidad de Cádiz
58 PUBLICATIONS **330** CITATIONS
SEE PROFILE

Concha Fernández-Lorenzo
Universidad de Cádiz
66 PUBLICATIONS **468** CITATIONS
SEE PROFILE

Jesús Idígoras
Universidad Pablo de Olavide
23 PUBLICATIONS **183** CITATIONS
SEE PROFILE

Juan A Anta
Universidad Pablo de Olavide
109 PUBLICATIONS **1,800** CITATIONS
SEE PROFILE

THE JOURNAL OF PHYSICAL CHEMISTRY Letters

LETTER

pubs.acs.org/JPCL

Direct Estimation of the Electron Diffusion Length in Dye-Sensitized Solar Cells

J. Navas,[†] E. Guillén,[‡] R. Alcántara,[†] C. Fernández-Lorenzo,[†] J. Martín-Calleja,[†] G. Oskam,[§] J. Idígoras,[‡] T. Berger,[‡] and J. A. Anta*[,‡]

[†]Departamento de Química Física, Universidad de Cádiz, 11510, Cádiz, Spain

[‡]Departamento de Sistemas Físicos, Químicos y Naturales, Universidad Pablo de Olavide, 41013 Sevilla, Spain

[§]Departamento de Física Aplicada, CINVESTAV-IPN, Mérida, Yucatán 97310, México

Supporting Information

ABSTRACT: The diffusion length is a key parameter that controls the electron collection efficiency in dye-sensitized solar cells (DSCs). In this work, we carry out a direct estimation of this parameter by means of the laser beam-induced current (LBIC) technique. The DSC devices are prepared on transparent conducting glass substrates, which were divided in two electrically isolated parts by means of a groove. The LBIC measurement is conducted by moving a highly focused laser spot over the DSC across the groove and monitoring the open-circuit voltage yielded by the solar cell. The resulting voltage profile can be fitted to a simple diffusion-recombination model such that the electron diffusion length can be extracted. Measurements carried out on DSC with various oxides (TiO_2/ZnO) and electrolytes (organic, ionic-liquid) yield diffusion lengths in the 10−35 μm range, with longer values found for higher illumination and for cells of better efficiency.

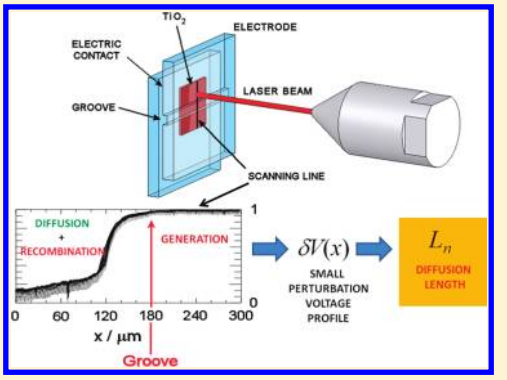

SECTION: Energy Conversion and Storage

Dye-sensitized solar cells (DSCs)[1,2] are considered one of the most interesting practical alternatives to conventional silicon-based solar cells, due to the simplicity of the fabrication process and the low cost of the semiconductors used in their fabrication (metal oxides such as TiO_2 and ZnO), while showing competitive efficiencies. In spite of the many papers published in the past two decades in the field of DSCs, some aspects of their functioning remain controversial,[3,4] such as, for example, the value of the electron diffusion length and the strategy that must be followed for its determination.[5−9]

The good performance of DSCs relies on the favorable dynamic competition[3,10,11] between the transport of photogenerated electrons through the semiconductor oxide nanostructure and recombination pathways that cause a reduction of the collection efficiency. For a DSC device to work efficiently, photogenerated electrons traveling through the semiconductor nanostructure should be collected with an efficiency of close to 100%. The electron diffusion length L_n represents the distance that electrons travel on average before recombining with an electron acceptor. Hence, efficient cells are characterized by L_n values that exceed the semiconductor film thickness.

The electron diffusion length is commonly determined from independent measurements of the electron diffusion coefficient D_n (quantifying electron transport kinetics) and the electron lifetime τ_n (quantifying electron recombination kinetics). The three quantities are related through the expression:[12] $L_n = (D_n\tau_n)^{1/2}$. Efficient experimental techniques employed to measure the transport and recombination characteristics are now used commonly in the literature, such as intensity modulated photocurrent and photovoltage spectroscopy (IMPS and IMVS)[13,14]and electrical impedance spectroscopy (EIS).[15−17] In addition, a method based on the measurement of the incident-photon-to-current efficiency (IPCE) and subsequent fitting to a numerical model has been proposed to obtain the electron diffusion length in DSCs.[18,19]

Very recently, a numerical method has been proposed to estimate the value of the electron diffusion length directly by averaging over random electron trajectories on an exponential distribution of trap energies.[20] However, there does not yet exist an equivalent experimental technique allowing for a direct estimation of the electron diffusion length in a DSC, based on the average distance that electrons travel in the film before recombination occurs. In this regard, Lana-Villareal and coworkers[21] reported on a novel approach to determine the electron diffusion length in a photoelectrochemical system with a long diffusion length. This method is based on a scanning

Received: March 12, 2011
Accepted: April 11, 2011
Published: April 15, 2011

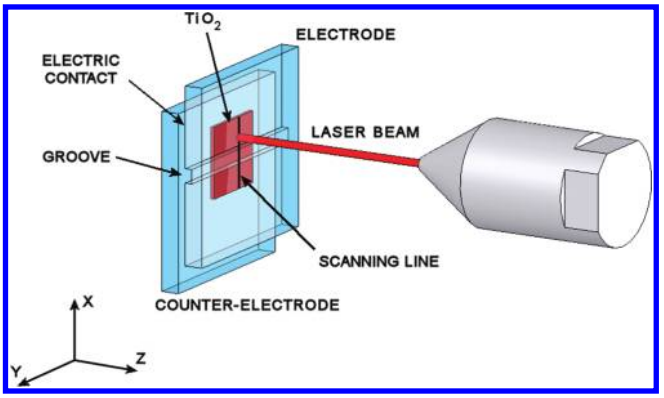

Figure 1. Illustration of the experimental setup utilized in this work. The laser beam is moved across the groove along the *x*-axis, and the open-circuit photovoltage is measured along the scanning line. An additional unfocused monochromatic illumination (not shown) is used to create a bias voltage.

technique featuring a laser beam. The photoactive mesoporous TiO_2 film was deposited on a transparent conducting glass (TCO), where a thin line of conducting film was removed by making a groove. This results in two electrically isolated parts in such a way that photoexcitation on one of the parts would produce a voltage signal on the other part only if electron transport through the mesoporous TiO_2 film takes place. By moving the laser beam across the groove, a progressive decay of the open-circuit voltage was observed. This decay is a direct probe of the average distance that electrons can travel in the film before recombining, that is, the electron diffusion length. By fitting the decays to a simple diffusion-recombination model this parameter can be estimated for electrons traveling and reacting in the film.

In this letter we apply the laser beam-induced current (LBIC) technique[22−25] to estimate the electron diffusion length of a DSC.[26] The LBIC technique can be considered an analogous method to that of Lana-Villareal et al.[21] A typical LBIC experiment is based on the light excitation of sample spots in the device with a focused laser beam (See Figure 1 and Figure S1, Supporting Information). This makes it possible to obtain the photocurrent (under short-circuit conditions, or at a voltage) or the photovoltage (under open-circuit conditions) of a solar cell as a result of the photoexcitation of a limited region on the photoactive surface. The LBIC technique has been reported previously in the literature to characterize solid-state solar cells[23,27,28] including the determination of the diffusion length in silicon-based solar cells.[29] It has been also applied recently to characterize DSCs, and photoconversion maps of operational devices have been obtained.[24,25]

With the aim of comparing devices with different performance, presumably with distinct characteristic diffusion lengths, we have studied two solar cell configurations: (1) mesoporous TiO_2 with organic solvent electrolyte and (2) mesoporous ZnO with ionic liquid (solvent-free) electrolyte, both sensitized with the N719 dye. Two different mesoporous films were used for TiO_2 (commercial paste from Solaronix and nanocrystalline TiO_2 synthesized by hydrothermal procedures). Details of the experimental procedure utilized to fabricate the devices can be found in previous reports[25,30] and in the Supporting Information. No special optimization procedures have been implemented to increase the efficiency since these devices are taken as benchmarks to test the feasibility of the method. It must be noted that the sensitivity of the method is especially critical for short diffusion lengths, as those expected for low efficiency devices.

As mentioned above, the mesoporous films analyzed in the LBIC experiment were deposited on modified TCO electrodes with two electrically isolated parts separated by a groove fabricated by laser ablation and with an approximate width of 2 mm (see Figure 1). The laser beam (see details in the Supporting Information) was focused on the photoactive surface and then moved along the *x*-axis (lateral resolution: 1 μm). The light intensity profile of the focused laser beam was Gaussian with a spot size of 3 μm (full width at half-maximum). The solar cell is held under open-circuit conditions, and the resulting photovoltage is measured along the scanning line. For some of the measurements, a uniform illumination is applied to produce a constant bias voltage in the entire scanned area. For this, a solid state laser emitting at 671 nm with a nominal power of 100 mW is used as illumination source. This illumination is unfocused and covers the whole active area of the solar cell.

In all measurements, a progressive decay of the open-circuit photovoltage is observed when the laser beam moves from the electrically contacted region to the isolated part of the solar cell (see Figure 2). As mentioned above, this decay is a direct probe of the average distance that electrons can travel through the nanocrystalline film before recombination. Thus, the photovoltage is observed to go from its maximum value to the base (background) value within a distance of 100 μm, suggesting that the diffusion length (defined as the average distance traveled) should be significantly smaller than this value. Measurements with three different excitation wavelengths lead to essentially the same results, which indicates that photonic dispersion has only a minor effect on the decays.

Following Lana-Villareal and co-workers,[21] we have fitted the experimental photovoltage decays to a diffusion−recombination model defined by the continuity equation for electrons[5,6,31−34] in the stationary state:

$$D_n \nabla^2 n(x,y,z) - \frac{n(x,y,z) - n_b}{\tau_n} = 0 \qquad (1)$$

where $n(x,y,z)$ is the concentration of electrons (number electron density), D_n is the effective electron diffusion coefficient, and τ_n is the effective electron lifetime. The following assumptions have been taken into account in eq 1:

1. n_b is a background electron density, which is assumed to be constant throughout the film. This background density is equal to the equilibrium dark density n_0 considered in ref 21 if no background illumination or electrical bias is applied to the film. The background electron density is an increasing function of the bias illumination as described below.
2. The recombination term is assumed to be linear with respect to the electron concentration. According to Bisquert and Mora-Seró,[5] this is a reasonable assumption if the excess electron density is a "small perturbation" with respect to the background term. A similar approach has been utilized by Jennings and Wang.[9] In any other situation, a reaction order different from 1 is applicable, and the electron diffusion length is not strictly defined.
3. There is no generation term since transport and recombination of the excess electron density takes places with respect to the background electron density. As described below, the

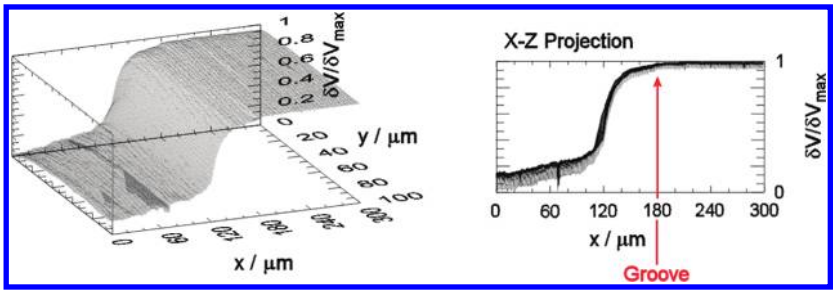

Figure 2. Photovoltage profiles (left) and projection on the $X-Z$ plane (right) obtained with the 632.8 nm laser for the TiO_2-based DSC studied in this work.

generation of excess electrons by the laser spot is introduced via a boundary condition.

4 The electron density considered in eq 1 includes, in principle, both trapped and free electrons. As a consequence, trapping effects should be taken into account both in the diffusion coefficient and the lifetime, which are taken here as effective magnitudes that depend on the value of the background density. Alternatively, a free density description (with a constant diffusion coefficient) is also adequate since we work under steady-state conditions. Both the total and the free density descriptions are shown to be equivalent in the stationary state.[31,33] The same values of the diffusion length are thus obtained with the method described here when a constant diffusion coefficient within the free density approach is applied.

In the LBIC experiment, the electron density is a function of the position (x,y,z) of the laser beam (see Figure 1). Hence, it is possible to solve eq 1 for a cylindrical geometry centered on the position of the laser spot (x_0,y_0) and imposing as a boundary condition the photogeneration rate G of electrons, which is a function of the light intensity. Details of this calculation, which we have reproduced in this work obtaining the same results, can be found in ref 21. The result for the density profile is

$$n(x,y,z) - n_b = \frac{G}{2\pi d D_n} K_0\left(\sqrt{\frac{(x-x_0)^2 + (y-y_0)^2}{D_n \tau_n}}\right) \quad (2)$$

where G is the electron generation rate (s^{-1}), d is the film thickness, and K_0 is the modified Bessel function of the second class and zero order.

The density profile (eq 2) is centered on the position of the laser spot (x_0,y_0) and shows an approximately exponential behavior with a radial geometry. The spatial range of the decay depends on $L_n = (D_n\tau_n)^{1/2}$, that is, the electron diffusion length. Hence, for systems with a long diffusion length, this decay is slower under stationary conditions, and, on the contrary, a short diffusion length produces a sharp profile centered at the position of the laser spot.

The increment of photovoltage with respect to the background voltage can be calculated via[31,33,35]

$$\delta V = \frac{k_B T}{e\alpha} \ln\left(\frac{n}{n_b}\right) \quad (3)$$

where k_B is the Boltzmann constant, T is the temperature, e is the elementary charge, n is the average density over the electrically connected surface, and α is the parameter that describes the energy depth of the trap distribution that accounts for electron trapping.[36−38] Note that if we use the free electron density instead of the total electron density in this theoretical description, no trapping factor is needed in eq 3. As mentioned above, the use of a free electron density description leads to the same results for the diffusion lengths.

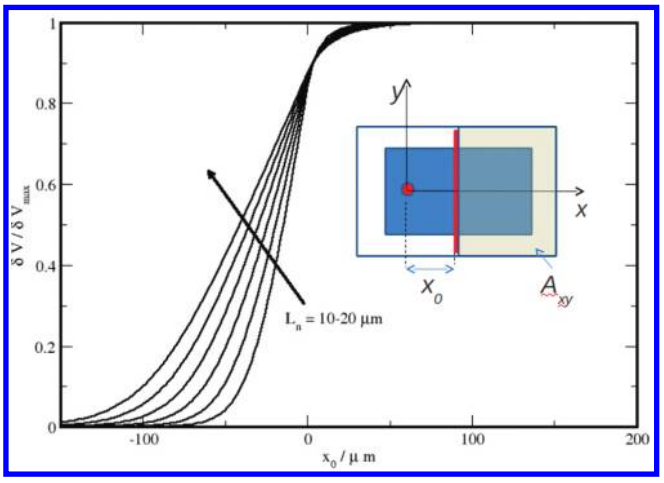

Figure 3. Photovoltage profiles for different diffusion lengths as obtained with the diffusion−recombination numerical model ($m = 1/\alpha = 1$, $D_n = 10-7$ cm^2 s^{-1}, $n_0 = 1015$ cm^{-3}, $d = 10$ μm, $a = 0.1$ cm, $A_{xy} = 2$ cm^2, $G = 1013$ cm^{-2} s^{-1}). The point $x_0 = 0$ represents the position of the groove. Parameters used in the modeling are shown in the figure.

Since the electron density is a function of position (x,y,z) via eq 2, the photovoltage measured as a function of the position of the laser beam will be obtained by averaging the electron density on an $x-y$ rectangle in the contacted part of the device and inserting the result in eq 3. Since the solution of eq 1 will depend on the position of the laser spot x_0, the resulting photovoltage will depend parametrically[21] on x_0:

$$\delta V(x_0) = \frac{k_B T}{e} 1/\alpha \ln\left[1 + \frac{1}{n_b}\left(\frac{1}{A_{xy}}\right)\int_{-a}^{a}\int_{x_0}^{x_0+a} (n(x,y,z) - n_b)\, dx\, dy\right] \quad (4)$$

where a (see Figure 3) defines the area of integration of eq 4 and A_{xy} is the total contacted area (note that a should be much longer than L_n to ensure convergence in the computation of the integral). In the present computations, we have used $a = 0.1$ cm and $A_{xy} = 2$ cm^2.

As the laser beam moves from the electrically contacted area toward the isolated area, less electrons will be "integrated" into eq 4 so that the photovoltage obtained will be smaller, hence generating a photovoltage profile. In Figure 3 the profiles obtained for different electron diffusion lengths in the 10−20 μm

dx.doi.org/10.1021/jz200340h | J. Phys. Chem. Lett. 2011, 2, 1045–1050

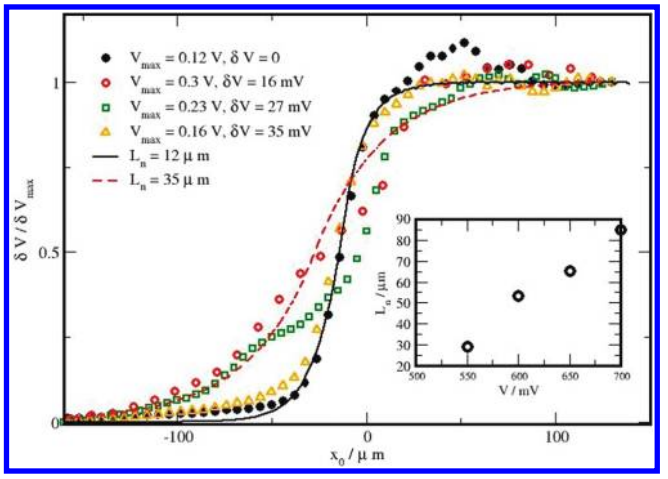

Figure 4. Photovoltage profiles for a TiO_2 (Solaronix) DSC (symbols) sensitized with the N719 dye and organic liquid electrolyte. This cell shows 5.6% efficiency under AM1.5, 1 sun conditions (see Supporting Information). The profiles were obtained with the 632.8 nm focused laser (intensities 5, 5, 3.2, and 1.4 μW for V_{max} = 0.12, 0.3, 0.23, and 0.16 V respectively) at different bias light intensities (intensities 0, 59, 22, and 9.8 μW for V_{max} = 0.12, 0.3, 0.23, and 0.16 V respectively). V_{max} and δV are, respectively, the maximum voltage obtained and the measured perturbation with respect to the bias voltage in each case. The lines stand for the best fit of these profiles to the numerical diffusion-recombination model ($m = 1/\alpha = 1$, $d = 10$ μm, $a = 0.1$ cm, A_{xy} = 2 cm^2). For clarity, only the fits for no bias ($D_n = 10^{-7}$ cm^2s^{-1}, n_0 = $10^{17}cm^{-3}$) and the highest bias ($D_n = 2\ 10^{-4}$ cm^2s^{-1}, $n_0 = 10^{22}$ cm^{-3}) are included. In the inset the diffusion lengths extracted from a impedance spectroscopy study performed on a DSC of the same configuration (see Supporting Information for details) are plotted. Note that the thickness of the film, as measured by profilometry, is approximately 10 μm. This is the value used to convert the impedance data to values of L_n in micrometers.

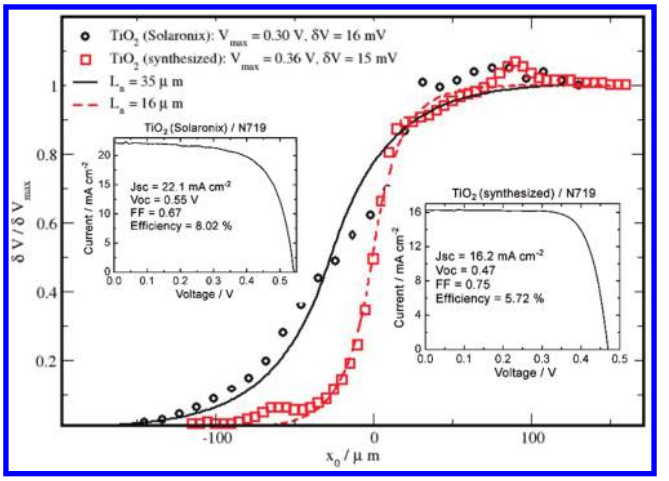

Figure 5. Average photovoltage profiles obtained with the 632.8 nm laser (intensities 5 and 3 μW for Solaronix and synthesized respectively) and bias illumination (intensity 59 μW) for TiO_2-based DSC studied in this work (symbols). The lines stand for the best fit of these profiles to the numerical diffusion-recombination model ($m = 1/\alpha = 1$, $d = 10$ μm, $a = 0.1$ cm, $A_{xy} = 2$ cm^2, $D_n = 10^{-4}$–$2\ 10^{-4}$ cm^2s^{-1}, $n_0 = 10^{21}$–10^{22} cm^{-3}). Note that the position of the groove ($x_0 = 0$) is arbitrary. In the insets the current–voltage curves of cells as obtained in situ with the same laser illuminating an area of 0.5 mm^2 with a power of 0.5 mW are shown. Monochromatic efficiencies for both devices are indicated in the figures.

range are presented. As expected, longer diffusion lengths produce slower decays. On the other hand, it must be noted that, according to the model, the diffusion-recombination effect is most visible once the laser spot is on the noncontacted part of the device. This feature provides an empirical method to compare experimental profiles from different devices for which the exact position of the groove cannot be easily located. The effect of other parameters on the profiles can be found in the Supporting Information (Figure S2). It is observed that increasing the diffusion coefficient (at constant L_n) or the background electron density also leads to "sharper" profiles as a consequence of the fact that electrons traveling faster, on average, will recombine at shorter distances. However, for values on the order of n_b = 10^{17}–10^{19} cm^{-3} and diffusion coefficients of D_n= 10^{-6}–10^{-4} cm^2 s^{-1}, the effect on the voltage decay of model parameters different from the diffusion length itself is very small. This feature provides assurance that the diffusion lengths extracted from the fitting of the experimental profiles correspond to true values of this parameter for the studied systems.

The experimental profiles of the three DSCs considered in this work are presented in Figures 4 and 5. The following points should be taken into account:

1 The experimental profiles are obtained by averaging over 100 scanning lines, that is, for different y-values. This is carried out by estimating the approximate position of the groove from simultaneous transmittance measurements for the different profiles.
2 Except in the case with no bias illumination, the excitation laser produces a perturbation with respect to the bias (background) voltage of 15–35 mV, similar to the small perturbations utilized in impedance spectroscopy studies.[17] This justifies the use of the linear approximation in the continuity eq 1 as explained above. However, the numerical model is found to work reasonably well for the largest perturbations as well.
3 Since the effective electron diffusion length is known to vary with electron density[9,39,40] (that is, with voltage or with light intensity), profiles for different cells are compared at a similar value of the bias voltage.
4 Experimentally, it is difficult to establish the precise location of the groove on the photovoltage decay. Hence, the position x_0 of the laser spot in eq 4 was taken as an additional fitting parameter to obtain the best agreement with the experimental data. In any case, this additional fitting strategy does not modify the estimated values of the diffusion length.

In Figure 4, the experimental voltage profiles obtained for a 0.64 cm^2 TiO_2 dye solar cell of 5.6% efficiency (AM1.5 illumination, 1 sun, see Supporting Information) at different values of bias illumination are shown. The best fits obtained from the application of the diffusion–recombination numerical model are plotted together with the experimental profiles. Diffusion lengths in the range of L_n = 12–35 μm are obtained. Furthermore, the electron diffusion length is clearly observed to increase with bias illumination. The agreement between the numerical model and the experimental profiles is reasonable. A parallel study on the same cell using impedance spectroscopy (see Inset in Figure 4 and the Supporting Information) provides diffusion lengths of the same order as those obtained from the LBIC method at similar values of the bias voltage (taking 10 μm for the film thickness). The values and the behavior with respect to bias

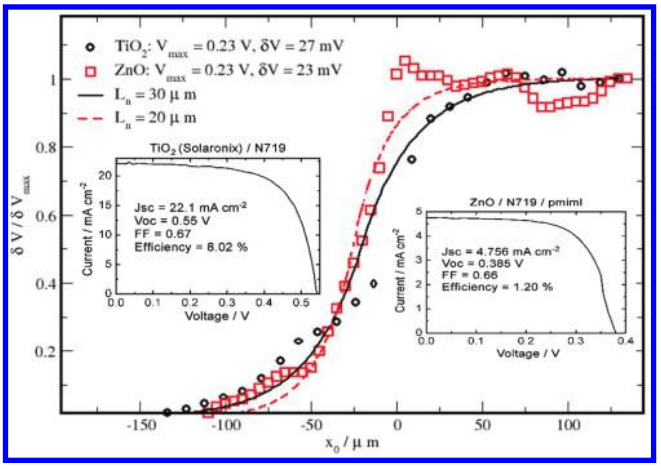

Figure 6. Average photovoltage profiles obtained with the 632.8 nm laser (intensities 5 and 8.6 μW for TiO_2 and ZnO respectively) and bias illumination (intensities 22 and 103 μW) for dye solar cells studied in this work (symbols). The lines stand for the best fit of these profiles to the numerical diffusion-recombination model ($m = 1/\alpha = 1$, $d = 10\ \mu$m, $a = 0.1$ cm, $A_{xy} = 2$ cm^2 $D_n = 3.4\ 10^{-5}$–$2\ 10^{-5}$ cm^{2}s^{-1}, $n_0 = 6.9\ 10^{20}$–10^{21} cm^{-3}). Note that the position of the groove ($x_0 = 0$) is arbitrary. In the insets the current–voltage curves of cells as obtained in situ with the same laser illuminating an area of 0.5 mm^2 with a power of 0.5 mW are shown. Monochromatic efficiencies for both devices are indicated in the figures.

voltage of the diffusion lengths found in this study are similar to data recently reported in the literature.[9,40,41]

It has to be noted that it was not possible to extend the LBIC data to larger bias, as the voltage perturbation profile (which is the magnitude actually used to extract the diffusion length) becomes very noisy, and it was not possible to fit the data to the numerical model accurately. On the other hand, the overlap of the cathode and transport resistances made it impossible to accurately extract the diffusion length from EIS at low voltages. This might be a problem in EIS measurements as reported previously.[14] However, the LBIC measurement can be extended to larger bias by fine-tuning the wavelengths and the intensities of the lasers used for bias and perturbation, respectively.

When applying the numerical model at different applied bias, it should be taken into account that the effective diffusion coefficient is an increasing function of the voltage. According to the multiple-trapping model, for an exponential distribution of trap states, we have[42,43]

$$D_n = D_0 \exp[(1-\alpha)eV/kT] \quad (5)$$

with the total density varying according to[33,35]

$$n_b = n_0 \exp[\alpha eV/kT] \quad (6)$$

where α is the aforementioned trap density parameter, and D_0 and n_0 are the dark equilibrium values of the electron diffusion coefficient and the electron density, respectively. In this study, we have used $\alpha = 0.33$,[44,45] and $D_0 = 10^{-7}$ cm^2/s, $n_0 = 10^{17}$ cm^{-3}.[21] However, as explained above, the use of different values for these parameters in the model is found to have little effect on the values of the estimated diffusion length.

In Figures 5 and 6, cells of different performance are directly compared at similar values of the bias voltage. In Figure 5 solar cells with two TiO_2 films (from Solaronix and from material synthesized in our laboratory) are compared. These cells show quite different efficiencies under monochromatic red light, although they are similar under white illumination (see Supporting Information for the AM1.5 curves). In general, lower photovoltages are obtained in the in situ measurement (as expected from a lower absorption coefficient of the dye in the red) and better photocurrents and fill factors. The better efficiency of the Solaronix cell in the in situ measurement appears to be correlated with the longer diffusion length found for this cell. In Figure 6 the comparison is performed between the most efficient TiO_2 cell and the ZnO-based solar cell. In this case, there is a larger difference in efficiency between the two devices, both under monochromatic and white light illumination. Again, a longer diffusion length is found for the most efficient cell, although the difference is not as high as in the comparison between the two TiO_2 cells. In this regard, it must be born in mind that the photocurrent does not depend only on electron collection but also on light harvesting and injection efficiency, and these two factors can be quite distinct for the ZnO-based solar cell.

In summary, we successfully combined an experimental approach based on LBIC measurements with a diffusion–recombination numerical model to directly estimate the value of the electron diffusion length in DSCs. Measurements carried out on a DSC with three alternative configurations lead to diffusion lengths in the 10–35 μm range, with longer diffusion lengths found for the cells with better photoconversion efficiency. The electron diffusion length is also observed to increase with light intensity, or higher voltage, corresponding to a higher electron density in the film.

■ ASSOCIATED CONTENT

Supporting Information. Experimental setup, dependence of the diffusion–recombination model on the different parameters, IV curves of the studied cells under AM1.5 illumination, and details of the impedance spectroscopy study. This material is available free of charge via the Internet http://pubs.acs.org.

■ ACKNOWLEDGMENT

We thank the Ministerio de Ciencia e Innovación of Spain for Project HOPE CSD2007-00007 (Consolider-Ingenio 2010) and CTQ2009-10477, a Ramon y Cajal fellowship and a FPU studentship, and Junta de Andalucía under Projects P07-FQM-02595, P07-FQM-02600, and P09-FQM-04938. G.O. acknowledges support from CONACyT under Grant No. 80002

■ REFERENCES

(1) O'Regan, B.; Gratzel, M. A Low-Cost, High-Efficiency Solar-Cell Based on Dye-Sensitized Colloidal TiO_2 Films. *Nature* **1991**, *353*, 737–740.
(2) Gratzel, M. Applied Physics - Solar Cells to Dye For. *Nature* **2003**, *421*, 586–587.
(3) Peter, L. M. Characterization and Modeling of Dye-Sensitized Solar Cells. *J. Phys. Chem. C* **2007**, *111*, 6601–6612.
(4) Hagfeldt, A.; Boschloo, G.; Sun, L.; Kloo, L.; Pettersson, H. Dye-Sensitized Solar Cells. *Chem. Rev.* **2010**, *110*, 6595–6663.
(5) Bisquert, J.; Mora-Seró, I. Simulation of Steady-State Characteristics of Dye-Sensitized Solar Cells and the Interpretation of the Diffusion Length. *J. Phys. Chem. Lett.* **2010**, *1*, 450–456.
(6) Villanueva-Cab, J.; Wang, H.; Oskam, G.; Peter, L. M. Electron Diffusion and Back Reaction in Dye-Sensitized Solar Cells: The Effect of Nonlinear Recombination Kinetics. *J. Phys. Chem. Lett.* **2010**, *1*, 748–751.
(7) Barnes, P. R. F.; Liu, L.; Li, X.; Anderson, A. Y.; Kisserwan, H.; Ghaddar, T. H.; Durrant, J. R.; O'Regan, B. C. Re-evaluation of Recombination Losses in Dye-Sensitized Cells: The Failure of Dynamic

Relaxation Methods to Correctly Predict Diffusion Length in Nanoporous Photoelectrodes. *Nano Lett.* **2009**, *9*, 3532–3538.

(8) Barnes, P. R. F.; Anderson, A. Y.; Koops, S. E.; Durrant, J. R.; O'Regan, B. C. Electron Injection Efficiency and Diffusion Length in Dye-Sensitised Solar Cells Derived from Incident Photon Conversion Efficiency Measurements. *J. Phys. Chem. C* **2009**, *113*, 12615.

(9) Jennings, J. R.; Li, F.; Wang, Q. Reliable Determination of Electron Diffusion Length and Charge Separation Efficiency in Dye-Sensitized Solar Cells. *J. Phys. Chem. C* **2010**, *114*, 14665–14674.

(10) Grätzel, M. Conversion of Sunlight to Electric Power by Nanocrystalline Dye-Sensitized Solar Cells. *J. Photochem. Photobiol., A* **2004**, *164*, 3–14.

(11) Hamann, T. W.; Jensen, R. A.; Martinson, A. B. F.; Ryswyk, H. V.; Hupp, J. T. Advancing beyond Current Generation Dye-Sensitized Solar Cells. *Energy Environ. Sci.* **2008**, *1*, 66–78.

(12) Harrick, N. J. Lifetime Measurements of Excess Carriers in Semiconductors. *J. Appl. Phys.* **1956**, *27*, 1439–1442.

(13) Peter, L. M.; Wijayantha, K. G. U. Electron Transport and Back Reaction in Dye Sensitised Nanocrystalline Photovoltaic Cells. *Electrochim. Acta* **2000**, *45*, 4543–4551.

(14) Wang, H.; Peter, L. M. A Comparison of Different Methods To Determine the Electron Diffusion Length in Dye-Sensitized Solar Cells. *J. Phys. Chem. C* **2009**, *113*, 18125–18133.

(15) Bisquert, J. Theory of the Impedance of Electron Diffusion and Recombination in a Thin Layer. *J. Phys. Chem. B* **2002**, *106*, 325–333.

(16) Fabregat-Santiagoa, F.; Bisquert, J.; Palomares, E.; Haque, S. A.; Durrant, J. R. Impedance Spectroscopy Study of Dye-Sensitized Solar Cells with Undoped Spiro-OMeTAD as Hole Conductor. *J. Appl. Phys.* **2006**, *100*, 034510–034517.

(17) Fabregat-Santiago, F.; Bisquert, J.; Garcia-Belmonte, G.; Boschloo, G.; Hagfeldt, A. Influence of Electrolyte in Transport and Recombination in Dye-Sensitized Solar Cells Studied by Impedance Spectroscopy. *Sol. Energy Mater. Sol. Cells* **2005**, *87*, 117–131.

(18) Barnes, P. R. F.; Anderson, A. Y.; Koops, S. E.; Durrant, J. R.; O'Regan, B. C. Electron Injection Efficiency and Diffusion Length in Dye-Sensitized Solar Cells Derived from Incident Photon Conversion Efficiency Measurements. *J. Phys. Chem. C* **2009**, *113*, 1126–1136.

(19) Halme, J.; Boschloo, G.; Hagfeldt, A.; Lund, P. Spectral Characteristics of Light Harvesting, Electron Injection, and Steady-State Charge Collection in Pressed TiO_2 Dye Solar Cells. *J. Phys. Chem. C* **2008**, *112*, 5623–5637.

(20) Gonzalez-Vazquez, J. P.; Anta, J. A.; Bisquert, J. Determination of the Electron Diffusion Length in Dye-Sensitized Solar Cells by Random Walk Simulation: Compensation Effects and Voltage Dependence. *J. Phys. Chem. C* **2010**, *114*, 8552–8558.

(21) Lana-Villarreal, T.; Monllor-Satoca, D.; Gómez, R.; Salvador, P. Determination of Electron Diffusion Lengths in Nanostructured Oxide Electrodes from Photopotential Maps Obtained with the Scanning Microscope for Semiconductor Characterization. *Electrochem. Commun.* **2006**, *8*, 1784–1790.

(22) Martin, J.; Fernandez-Lorenzo, C.; Poce-Fatou, J. A.; Alcantara, R. A Versatile Computer-Controlled High-Resolution LBIC System. *Prog. Photovoltaics* **2004**, *12*, 283–295.

(23) Müller, M. H.; Rinio, M LBIC Investigations of the Lifetime Degradation by Extended Defects in Multicrystalline Solar Silicon. *Solid State Phenom.* **1996**, *63/64*, 115–122.

(24) Guillen, E.; Casanueva, F.; Anta, J. A.; Vega-Poot, A.; Oskam, G.; Alcantara, R.; Fernandez-Lorenzo, C.; Martin-Calleja, J. Photovoltaic Performance of Nanostructured Zinc Oxide Sensitised with Xanthene Dyes. *J. Photochem. Photobiol. A: Chem.* **2008**, *200*, 364–370.

(25) Navas, J.; Alcántara, R.; Fernández-Lorenzo, C.; Anta, J.-A.; Guillén, E.; Martín-Calleja, J. Improving Photoresponse Characterization of Dye-Sensitized Solar Cells: Application to the Laser Beam-Induced Current Technique. *Meas. Sci. Technol.* **2010**, *21*, 075702.

(26) We use here the name "laser beam-induced current" because it is the name commonly used in the previous literature for this positional technique, and it is possible in fact to measure currents instead of voltages. However, we report here voltages rather than currents because it is more straightforward to model the profiles at open-circuit than at short circuit.

(27) Acciarri, M.; Binetti, S.; Racz, A.; Pizzini, S.; Agostinelli, G. Fast LBIC In-Line Characterization for Process Quality Control in the Photovoltaic Industry. *Sol. Energy Mater. Sol. Cells* **2002**, *72*, 417–424.

(28) Kaminski, A.; Breitenstein, O.; Boyeaux, J. P.; Rakotoniaina, P.; Laugier, A. Light Beam Induced Current and Infrared Thermography Studies of Multicrystalline Silicon Solar Cells. *J. Phys.: Condens. Matter* **2004**, *16*, S9–S18.

(29) Yamamoto, Y.; Ishikawa, Y.; Hatayama, T.; Uraoka, Y.; Fuyuki, T. Numerical Analysis of Bulk Diffusion Length in Thin-Film c-Si Solar Cells. *Sol. Energy Mater. Sol. Cells* **2003**, *75*, 433–438.

(30) Guillen, E.; Idigoras, J.; Berger, T.; Anta, J.; Fernandez-Lorenzo, C.; Alcantara, R.; Navas, J.; Martin-Calleja, J. ZnO-Based Dye Solar Cell with Pure Ionic-Liquid Electrolyte and Organic Sensitizer: The Relevance of the Dye-Oxide Interaction in an Ionic-Liquid Medium. *Phys. Chem. Chem. Phys.* **2011**, *13*, 207–213.

(31) Villanueva-Cab, J.; Oskam, G.; Anta, J. A. A Simple Numerical Model for the Charge Transport and Recombination Properties of Dye-Sensitized Solar Cells: A Comparison of Transport-Limited and Transfer-Limited Recombination. *Sol. Energy Mater. Sol. Cells* **2010**, *94*, 45–50.

(32) Villanueva, J.; Anta, J. A.; Guillén, E.; Oskam, G. Numerical Simulation of the Current−Voltage Curve in Dye-Sensitized Solar Cells. *J. Phys. Chem. C* **2009**, *113*, 19722–19731.

(33) Anta, J. A.; Casanueva, F.; Oskam, G. A Numerical Model for Charge Transport and Recombination in Dye-Sensitized Solar Cells. *J. of Phys. Chem. B* **2006**, *110*, 5372–5378.

(34) Halme, J.; Vahermaa, P.; Miettunen, K.; Lund, P. Device Physics of Dye Solar Cells. *Adv. Mater.* **2010**, *22*, E210–E234.

(35) Frank, A. J.; Kopidakis, N.; van de Lagemaat, J. Electrons in Nanostructured TiO_2 Solar Cells: Transport, Recombination and Photovoltaic Properties. *Coord. Chem. Rev.* **2004**, *248*, 1165–1179.

(36) Nelson, J. Continuous-Time Random-Walk Model of Electron Transport in Nanocrystalline TiO_2 Electrodes. *Phys. Rev. B* **1999**, *59*, 15374–15380.

(37) Nelson, J. Diffusion-Limited Recombination in Polymer−Fullerene Blends and Its Influence on Photocurrent Collection. *Phys. Rev. B* **2003**, *67*, 155209.

(38) Bisquert, J.; Fabregat-Santiago, F.; Mora-Sero, I.; Garcia-Belmonte, G.; Barea, E. M.; Palomares, E. A Review of Recent Results on Electrochemical Determination of the Density of Electronic States of Nanostructured Metal-Oxide Semiconductors and Organic Hole Conductors. *Inorg. Chim. Acta* **2008**, *361*, 684–698.

(39) Peter, L. M.; Wijayantha, K. G. U. Intensity Dependence of the Electron Diffusion Length in Dye-Sensitised Nanocrystalline TiO_2 Photovoltaic Cells. *Electrochem. Commun.* **1999**, *1*, 576–580.

(40) Bisquert, J.; Fabregat-Santiago, F.; Mora-Seró, I.; Garcia-Belmonte, G.; Giménez, S. Electron Lifetime in Dye-Sensitized Solar Cells: Theory and Interpretation of Measurements. *J. Phys. Chem. C* **2009**, *113*, 17278–17290.

(41) Wang, M.; Chen, P.; Humphry-Baker, R.; Zakeeruddin, S. M.; Gratzel, M. The Influence of Charge Transport and Recombination on the Performance of Dye-Sensitized Solar Cells. *ChemPhysChem* **2009**, *10*, 290–299.

(42) Bisquert, J.; Vikhrenko, V. S. Interpretation of the Time Constants Measured by Kinetic Techniques in Nanostructured Semiconductor Electrodes and Dye-Sensitized Solar Cells. *J. Phys. Chem. B* **2004**, *108*, 2313–2322.

(43) Anta, J. A.; Mora-Sero, I.; Dittrich, T.; Bisquert, J. Interpretation of Diffusion Coefficients in Nanostructured Materials from Random Walk Numerical Simulation. *Phys. Chem. Chem. Phys.* **2008**, *10*, 4478–4485.

(44) Fabregat-Santiago, F.; Randriamahazaka, H.; Zaban, A.; Garcia-Canadas, J.; Garcia-Belmonte, G.; Bisquert, J. Chem.ical Capacitance of Nanoporous-Nanocrystalline TiO_2 in a Room Temperature Ionic Liquid. *Phys. Chem. Chem. Phys.* **2006**, *8*, 1827–1833.

(45) Anta, J. A.; Mora-Sero, I.; Dittrich, T.; Bisquert, J. Dynamics of Charge Separation and Trap-Limited Electron Transport in TiO_2 Nanostructures. *J. Phys. Chem. C* **2007**, *111*, 13997–14000.